RESEARCH ARTICLE
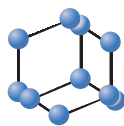
Peptide R18H from BRN2 Transcription Factor POU Domain Displays Antitumor Activity *In Vitro* and *In Vivo* and Induces Apoptosis in B16F10-Nex2 Cells

Fernanda F.M. da Cunha[1], Katia C.U. Mugnol[2], Filipe M. de Melo[3], Marta V.S.Q. Nascimento[2], Ricardo A. de Azevedo[4], Raquel T.S. Santos[1], Jéssica A. Magalhães[5], Danilo C. Miguel[6], Dayane B. Tada[7], Renato A. Mortara[8], Luiz R. Travassos[4] and Denise C. Arruda[1,*]

[1]*Núcleo Integrado de Biotecnologia (NIB), Universidade de Mogi das Cruzes, UMC, Mogi das Cruzes, SP, Brazil;* [2]*Centro Interdisciplinar de Investigação Bioquímica (CIIB) Universidade de Mogi das Cruzes, UMC, Mogi das Cruzes, SP, Brazil;* [3]*Departamento de Imunologia, Escola Paulista de Medicina, Universidade Federal de São Paulo (UNIFESP), São Paulo, SP, Brazil;* [4]*Unidade de Oncologia Experimental (UNONEX), Escola Paulista de Medicina, Universidade Federal de São Paulo (UNIFESP), São Paulo, SP, Brazil;* [5]*Laboratório de Nanomateriais e Nanotoxicologia, Instituto de Ciência e Tecnologia, Universidade Federal de São Paulo (UNIFESP), São José dos Campos, SP, Brazil;* [6]*Departamento de Biologia Animal, Instituto de Biologia, Universidade Estadual de Campinas (UNICAMP), Campinas, SP, Brazil;* [7]*Laboratório de Nanomateriais e Nanotoxicologia, Instituto de Ciência e Tecnologia, Universidade Federal de São Paulo (UNIFESP), São José dos Campos, SP, Brazil;* [8]*Departamento de Microbiologia, Imunologia e Parasitologia, Escola Paulista de Medicina, Universidade Federal de São Paulo (UNIFESP), São Paulo, SP, Brazil*

Abstract: *Background*: BRN2 transcription factor is associated with the development of malignant melanoma. The cytotoxic activities and cell death mechanism against B16F10-Nex2 cells were determined with synthetic peptide R18H derived from the POU domain of the BRN2 transcription factor.

Objective: To determine the cell death mechanisms and *in vivo* activity of peptide R18H derived from the POU domain of the BRN2 transcription factor against B16F10-Nex2 cells.

Methods: Cell viability was determined by the MTT method. C57Bl/6 mice were challenged with B16F10-Nex2 cells and treated with R18H. To identify the type of cell death, we used TUNEL assay, Annexin V and PI, Hoechst, DHE, and determination of caspase activation and cytochrome c release. Transmission electron microscopy was performed to verify morphological alterations after peptide treatment.

Results: Peptide R18H displayed antitumor activity in the first hours of treatment and the EC50% was calculated for 2 and 24h, being 0.76 ± 0.045 mM and 0.559 ± 0.053 mM, respectively. After 24h apoptosis was evident, based on DNA degradation, chromatin condensation, increase of superoxide anion production, phosphatidylserine translocation, activation of caspases 3 and 8, and release of extracellular cytochrome c in B16F10-Nex2 cells. The peptide cytotoxic activity was not affected by necroptosis inhibitors and treated cells did not release LDH in the extracellular medium. Moreover, *in vivo* antitumor activity was observed following treatment with peptide R18H.

Conclusion: Peptide R18H from BRN2 transcription factor induced apoptosis in B16F10-Nex2 and displayed antitumor activity *in vivo*.

1. BACKGROUND

Although malignant melanoma may not be the most common type of skin cancer, it is associated with high mortality due to the great propensity to metastasize. According to statistics by the American Cancer Society, it was estimated that in 2018 alone, about 9,320 people will die of melanoma in USA [1]. Moreover, malignant melanoma incidence has increased significantly in the world since the early 1970s, at an average rate of 4% per year [2].

The existence of cells resistant to conventional treatment validates further studies on new drugs for the treatment of melanoma. The same idea is valid to other types of cancer, as described in an extensive review by Block *et al*. [3]. In this study, the authors refer to a broad-spectrum approach to cancer prevention and treatment as an alternative to combine different agents of low toxicity aiming at

*Address correspondence to this author at the Núcleo Integrado de Biotecnologia (NIB), Universidade de Mogi das Cruzes, UMC, Mogi das Cruzes, SP, Brazil; Tel: +55 11 47987089; E-mail: denisearr@gmail.com

maximizing therapy efficiency and minimize resistance, relapses and costs.

Some studies suggest that melanoma resistance is probably caused by a deregulation of apoptotic processes since the rates of apoptosis in the more advanced stages of the disease are very low. Thus, the search for the development of molecules that interfere with the process of cell death has aroused interest as a therapeutic possibility [4, 5].

Bioactive peptides with antitumor activity have been studied for their capacity to induce cancer cell death. Several studies have shown that peptides can cause necrosis [6], apoptosis [7-10], necroptosis [11], autophagy [12], or even two kinds of cell death at the same time, for example, the association of apoptosis and autophagy in melanoma cells as induced by AC1001-H3 peptide [13].

BRN2 protein was originally found in neuronal cells and is involved in the development of the central nervous system and neurons, but it was also expressed in melanocytes [14]. The protein may be overexpressed in malignant melanoma and consequently induce proliferation and cellular invasion [15-17]. Activation of MAPK pathways, usually by BRAF mutation or Akt-PI3K pathway, as well as nuclear accumulation of beta-catenin, are common events in melanoma cells. These pathways increase the expression of BRN2 [16, 18, 19], disclosing the importance of this protein in melanoma cells.

The use of peptides derived from transcription factors could be a new strategy to interfere with vital signaling that permits melanoma progression. Peptides from POU domain of BRN2, which contains a DNA binding sequence, might compete with the protein for the DNA binding site, as well as induce cell death in melanoma cells. We have tested peptide R18H from POU domain of BRN2 transcription factor in B16F10-Nex2 cells. Presently, we show that peptide R18H induced apoptosis in B16F10-Nex2 tumor cells. Furthermore, the peptide caused a reduction in the development of pulmonary nodules in melanoma metastatic model.

2. METHODS

2.1. Cell Lines

B16F10, a syngeneic murine melanoma cell line in C57BL/6 mice, was originally obtained from the Ludwig Institute for Cancer Research, São Paulo. The clone B16F10-Nex2, a murine melanoma subline, was established at the Experimental Oncology Unit, Federal University of São Paulo, UNIFESP, as described elsewhere [20]. The fully characterized B16F10-Nex2 melanoma cell line was deposited in the 'Banco de Células do Rio de Janeiro' (BCRJ, Brazil), no. 0342.

The human melanoma cell lines A2058 and SK-MEL 25 were provided by the Ludwig Institute for Cancer Research, São Paulo, Brazil. The human melanoma cell line A375 was provided by 'Banco de Células do Rio de Janeiro' (BCRJ, Brazil), no. 0278.

The cells were grown in RPMI 1640 medium (Invitrogen) supplemented with 10 mM HEPES (Sigma Aldrich), 24 mM sodium bicarbonate, 40 mg/liter gentamicin (Hipolabor, Sabará, MG, Brazil), pH 7.2, and 10% fetal bovine serum (FBS Cultilab, Campinas, SP, Brazil in culture flasks at 37°C in a humidified atmosphere with 5% CO_2.

Nontumor J774 1.6 macrophage cell line (BCRJ, no. 0273) was used as a natural control and was a gift from Prof. Dr. Edgar J. P. Gamero from Federal University of Mato Grosso do Sul. Human

foreskin fibroblast (Fibro RP) were donated by Luis F. Lima Reis, Hospital Sirio-Libanês, São Paulo. These cell lineages were maintained in DMEM supplemented as described above, at 37°C in a humidified atmosphere with 5% CO_2. Nontumor HUVEC Human Endothelial cells also were used as controls and were a gift from Prof. Dr. Júlio Scharfstein of Federal University of Rio de Janeiro. This cell line was maintained in RPMI supplemented as described above, also at 37°C in a humidified atmosphere with 5% CO_2. maintained in supplemented as described above, also at 37°C in a humidified atmosphere with 5% CO_2.

2.2. Primary Cell

Cytotoxicity was also determined for BALB/c mice bone-marrow-derived macrophages. Briefly, bone marrow cells were differentiated into macrophages after 7 days as previously described [21] and cultured in 96-well plates at 37°C, 5% CO_2 in RPMI 1641 medium. Approximately 5×10^6 macrophages were incubated with increasing concentrations of 0.5 and 0.75 mM for 24h. The viability was assessed by the MTT method [13]. The protocol for tibia and femur extraction from BALB/c mice was approved by the Ethical Committee for Animal Experimentation of the Biology Institute of UNICAMP (#4535-1/2017).

2.3. Hemolysis Test in Human Red Blood Cells

5 mL of blood collected in a tube containing EDTA was centrifuged at 980 x *g* for 15 min. Plasma was withdrawn and red blood cells washed 3x with 0.9% NaCl (1:1) and centrifuged at 980 x *g* for 5 min. Red blood cells were treated with peptide R18H diluted in PBS at concentrations of 0.5 and 0.75 mM and incubated for 30 min at room temperature with gentle agitation and centrifuged at 980 x *g* for 3 min. The supernatant was removed and analyzed by spectrophotometer at 540 nm. As a positive lysis control, red blood cells were resuspended in distilled water (1:20) and a negative control, red blood cells were resuspended in PBS (1:20). Experiments were performed in triplicate [22].

2.4. Peptides

Peptide R18H (RKKRTSIEVSVKGALESH) and peptide A12G (AKQFKQRRIKLG) from transcription factor BRN2 were synthesized by Peptide 2.0 (Chantilly, VA) and alternatively by AminoTech Pesquisa e Desenvolvimento (São Paulo, SP). R18H was diluted in RPMI 1640 medium for *in vitro* experiments and in PBS for *in vivo* experiments.

2.5. Cell Viability Assay

Cells were cultivated (5×10^3/well) in RPMI medium in 96-well plates at 37°C in a humidified atmosphere containing 5% CO_2. After 24h, cells were incubated for 2 or 24h with R18H at different concentrations: 0.06, 0.12, 0.25, 0.50, 0.75 and 1 mM at 37°C and the EC50% values determined for 2 and 24h. Cells were treated with 0.5 and 0.75 mM peptide for 30 min, 1, 2, 4, 6, 12 and 24h at 37°C to generate a time curve. After incubation with the peptide, 5μL of MTT (3-[4,5-dimethylthiazol-2-yl]-2,5-diphenyltetrazolium bromide) (Sigma-Aldrich, St. Louis, MO) solution (5 mg/mL) was added to each well and incubated at 37°C. After 5h, SDS 10% was directly added and incubated overnight at 37°C and absorbance measured using an automated spectrophotometric plate reader (Synergy H1 hybrid reader) at 570 nm. Alternatively, the cells were collected with trypsin and counted in a Neubauer chamber using Trypan blue exclusion test. All experi-

ments were performed in triplicate, in three independent experiments. The viability was expressed as percent values [13].

Cell viability after treatment with R18H was also tested in presence of specific inhibitors of apoptosis and necroptosis as well as anion superoxide. B16F10-Nex2 (5×10^3/well) cells were cultivated in 96-well plates under normal conditions. Cells were previously incubated with 2 μM Z-VAD [23], 50 μM necrostatin [24], or 10 mM N-acetyl L-cysteine [25] for 2 or 3h, all inhibitors being tested in independent experiments. Afterward, cells were thereafter treated with 0.75 mM R18H for 2 or 24 hours in the presence of inhibitors. Untreated cells, cells treated only with R18H, treated with inhibitors or treated with R18H in presence of inhibitors, were collected with trypsin and counted in a Neubauer chamber using Trypan blue exclusion test. All experiments were performed in triplicate, in three independent experiments and the results are expressed as percent values.

2.6. TUNEL Assay

DNA fragmentation after treatment with R18H was analyzed by fluorescence microscopy using TUNEL assay ("*In Situ* Cell Death Detection kit, AP" - Roche Molecular Biochemicals, Mannheim, Germany) [26]. TUNEL assay was performed according to the manufacturer's instructions. B16F10-Nex2 cells (10^4/well) were cultivated in 24-well plates on round glass coverslips and treated with 0.75 mM R18H for 2 or for 24h with 0.8 mM, both at 37°C. Cells were fixed with 3.5% formaldehyde for 30 min and permeabilized with Triton X-100 0.1% for 30 min at room temperature. Cells were then incubated with 50 μL of TUNEL reaction mixture (peptide treated, positive control, and untreated cells) for 1h, at 37°C, protected from light. These cells were also stained with 10 μg/mL DAPI (Invitrogen) for 10 min. The cells were imaged by fluorescence microscopy in an Olympus BX-51 microscope using a 60x oil immersion 1.4 N.A. objective. Images were analyzed with ImageJ.

2.7. Chromatin Condensation

Chromatin Condensation was observed by fluorescence microscopy in treated cells with peptide R18H and stained with Hoechst 33342. B16F10-Nex2 cells (10^4/well), were cultivated overnight on round glass coverslips in 24-well plates. Cells were treated with 0.8 mM R18H for 2h or 0.75 mM R18H for 24h, at 37°C, washed with PBS and fixed with 2% formaldehyde for 30 min at room temperature. Cells were washed with PBS and stained with 2 μM Hoechst 33342 (Invitrogen) for 10 min. Cells were visualized in an Olympus BX-51 fluorescence microscope with a 60x oil immersion 1.4 N.A. objective. Images were processed with ImageJ [27].

2.8. Phosphatidylserine Translocation

B16F10-Nex2 cells (5×10^5) were cultivated with 0.5 mM R18H for 2 or 24h at 37°C and 5% CO_2. Treated and untreated cells (1×10^6) were harvested with trypsin and incubated with binding buffer (10 mM HEPES pH 7.5, 140 mM NaCl and 2.5 mM $CaCl_2$) in the presence of propidium iodide and annexin V (Annexin V-FITC Apoptosis Detection kit; Sigma, Saint Louis, MO) [28] for 10 min at room temperature and analyzed by flow cytometry (FACS Canto II, BD, Franklin Lakes, NJ) with Cell Quest software.

2.9. Superoxide Anions Production

The increase in superoxide anions production after the treatment with R18H was determined by dihydroethidium (DHE) assay

according to the manufacturer's instructions (Invitrogen, Carlsbad, CA) and analyzed as previously described [9]. B16F10-Nex2 cells (10^4/well) were grown in 24-well plates, treated with 0.75 mM R18H for 2h or for 24h with 0.8 mM, at 37°C. As a positive control, cells were treated with 5 mM H_2O_2 for 20 min. Treated and untreated cells were incubated with 5 μM DHE for 30 min at room temperature. Cells were immediately analyzed by fluorescence microscopy in an Olympus IX-70 microscope using a 40x objective. DHE-stain DNA was observed by the red fluorescence. Images were analyzed with ImageJ.

2.10. Caspase Activation

Activation of caspases 3, 8 and 9, was determined by the Apotarget Caspase Colorimetric Protease Assay Sampler Kit (Invitrogen, Camarillo, CA), according to the manufacturer's instructions. B16F10-Nex2 cells (3×10^5/well) were cultivated in 6-well plates and treated with 0.75 mM R18H for 30 min at 37°C. After washing, cells were harvested, pelleted and resuspended in 50 μL of chilled Cell Lysis Buffer and incubated in ice for 10 min. Cell lysates were centrifuged at 10,000 g for 1 min and the supernatants transferred to fresh tubes. Bradford method was used to determine protein concentration and the extract was diluted to 3 mg/mL. An equal volume (50 μL) of 2x Reaction Buffer with 10 mM DTT was added to each sample. Samples were incubated with 200 μM of the substrates, DEVD-*p*NA (caspase-3), IETD-*p*NA (caspase-8), and LEHD-*p*NA (caspase-9), at 37°C for 2h in a 96-well plate. Light absorption by free para-nitroaniline (*p*NA) as a result of synthetic substrate-*p*NA cleavage by caspases was quantified using a microplate reader (Synergy H1 wybrid reader) at 405 nm [29].

2.11. Extracellular Release of Cytochrome c

Cytochrome c is an important marker of cell death and in this study we detected and quantified this protein in the extracellular medium as a more specific and early marker of the apoptotic process. After a period of cell incubation with the peptide, extracellular medium was collected and centrifuged at 2500 x g for 5 min at 4°C and the supernatant examined in the Enzyme-Linked Immunosorbent Assay (ELISA-Invitrogen® kit KHO1051). Samples, controls and standards (a serial dilution of the cytochrome c with pre-determined concentration) were added to wells of a plate containing monoclonal antibody specific for cytochrome c capture. After adding 100 μL of each sample into its respective well, the plate was incubated for two hours at room temperature. After incubation, the solution was decanted, the plate washed four times (washing cycle) and 100 μL of cytochrome c-biotin conjugate solution added in the wells. After incubation for another hour at room temperature, a new washing cycle was performed followed by the addition of 100 μL of Streptavidin-HRP working solution. After another 30 min at the same temperature condition, a last washing cycle was performed and 100 μL of stabilized chromogen added followed by a new incubation for 30 min in the dark. After this, 100 μL of Stop Solution was added and then absorbance was read at 450 nm against a blank (BioTek Elx800). A standard curve for cytochrome c was used to determine the concentration of each sample [30].

2.12. Plasma Membrane Permeabilization

To determine plasma membrane permabilization, cells were stained with the nuclear stain Propidium Iodide (PI). B16F10-Nex2 cells (10^4) were cultivated in 24 well plates. Cells were treated with 0.75 mM R18H for 2h or for 24h with 0.8 mM, washed with PBS

and immediately stained with 2 µg/mL PI (Sigma, Saint Louis, MO) and with 2 µM Hoechst 33342 (Invitrogen) for 10 min. Cells were visualized in an Olympus IX-70 fluorescence microscope using a 40x objective. Images were processed with ImageJ. As a positive control, cells were treated with 1 M acetic acid for 1h [28].

2.13. Determination of Extracellular LDH Release

Lactate dehydrogenase activity, a conventional method to measure cellular injury, was performed using LDH Activity Assay Kit Sigma Aldrich® (MAK066). The extracellular medium after the period of cell treatment with the peptide was collected and centrifuged at 2,500 x g for 5 min at 4°C and the supernatant used in this assay. A NADH standard curve was added in duplicate into a 96-wells plate (0, 2, 4, 6, 8 and 10 µL) with LDH assay buffer to a final volume of 50 µL (final concentrations were 0, 2.5, 5, 7.5, 10 and 12.5 nM, respectively). Aliquots of 2 µL of each supernatant were added to 48 µL of the assay buffer. All wells received 50 µL of the master reaction mix. After 3 min at room temperature and in the dark, an initial measurement (T initial) of the absorbance at 450 nm (A450 initial) was taken. After that, the plate was incubated at 37°C taking measurements (A450) being taken every 5 min, always protecting from light. Measurements continued until the value of the most active sample was close or exceeded the end of the linear range of the standard curve. The penultimate reading, considered T final, To, was used to calculate enzyme activity. To calculate LDH activity, the initial A450 was subtracted from final A450 final and the value obtained compared to the standard curve to determine the amount of NADH generated. Absorbance was determined in an Absorbance Microplate Reader (BioTek Elx800) [30, 31].

2.14. Transmission Electron Microscopy

B16F10-Nex2 cells ($5x10^4$) were incubated with 1 mM R18H for 24h at 37°C and fixed in a solution of 2.5% glutaraldehyde and 2% formaldehyde in 0.1 M sodium cacodylate buffer, pH 7.2, at room temperature for 20h. Next, cells were washed in the same buffer for 10 min, fixed with 1% osmium tetroxide in 0.1 M cacodylate at pH 7.2 for 30 min, and washed with water for 10 min at room temperature Cells were then treated with an aqueous solution of 0.4% uranyl acetate for 30 min and washed with water for 10 min. Cells were dehydrated in graded ethanol (70, 90, and 100%), treated quickly with propylene oxide, and embedded in EPON. Ultra-thin sections from selected regions were collected on grids and stained in alcoholic 1% uranyl acetate and in lead citrate prior to examination in a Jeol 1200 EXII electron microscope (Tokyo, Japan) [13].

2.15. Confocal Microscopy

B16F10-Nex2 cells ($1x10^4$) were plated on round glass coverslips and incubated for 24h under normal cell growth conditions. Cells were washed with PBS and incubated for 30 min, 2h and 24h with 0.5 mM biotinylated R18H and then washed with PBS. Cells were fixed with 3.7% paraformaldehyde for 30 min, washed in PBS and then permeabilized in 0.1% Triton X-100 for 30 min followed by blocking for 1h with 150 mM NaCl, 50 mM Tris, and 0.25% BSA, all from Sigma-Aldrich. Cells were incubated for 1h in the dark at 4°C with streptavidin-AlexaFluor 488 conjugate (Invitrogen) diluted 1:200 in PBS. Cells were then washed and stained with 10 µg/ml DAPI (Invitrogen) for 10 min and rhodamine-phalloidin (Invitrogen) diluted 1:200 in PBS. Coverslips were mounted on slides with 4 µl of Vectashield (Sigma) and observed in a Confocal

Leica SP5 microscope with an 63x 1.4 oil objective; z-series was obtained according to sampling criteria built in the software and analyzed by ImageJ [9].

2.16. Treatment with R18H *in vivo* in the Melanoma Metastatic Model

Six- to eight-week-old male C57BL/6 mice were obtained from the animal house facility of University of Mogi das Cruzes (UMC, São Paulo, Brazil), kept in isolators with autoclaved water and food. Animal experiments were carried out in accordance with the UMC Ethics Committee for Animal Experimentation (11/015). Syngeneic B16F10-Nex2 cells ($5x10^5$) cells were injected (in 0.1 mL PBS) intravenously in the tail veins of mice (5 animals for group) and on the following day intraperitoneal treatment began for five alternate days with R18H (300 µg/day/mouse) [13]. The control group received the same volume of PBS. Ten days after the end of treatment, lungs were collected, photographed and the area of metastatic nodules was determined.

To determine R18H toxicity *in vivo*, the peptide diluted in 100 µL of PBS was administered intraperitoneally at 1 mg/day/mouse for 3 consecutive days. Control mice received 100 µL of PBS. Two days after the end of treatment, mice were euthanized. Heart, lung, spleen, liver, and kidneys of each mouse were removed for histology by hematoxylin-eosin staining of sections [9].

2.17. Statistical Analysis

The data were expressed as means ± standard deviation. Significant differences were assessed using ANOVA and p values < 0.05 were considered significant.

3. RESULTS

3.1. Cytotoxic Effect of Peptide R18H

The viability of B16F10-Nex2 cells after the treatment with R18H, derived from the POU domain of BRN2 transcription factor was determined. Cells were treated with increasing concentrations ranging from 0.06 to 1 mM, for either 2 or 24 hours. Untreated cells were incubated in the absence of peptide. Results showed a significant decrease in the viability of murine melanoma B16F10-Nex2 cells treated with peptide R18H for 2h (Fig. **1A**) or 24h (Fig. **1B**) as compared to untreated cells, showing a dose-response curve. The EC50% was determined for 2 and 24h, being 0.76 ± 0.045 mM and 0.559 ± 0.053 mM, respectively.

As a negative control we used another peptide derived from the POU domain of transcription factor Brn-2, peptide A12G. This peptide showed no antitumor effect in B16F10-Nex2, at 1 mM after 24h of treatment (Supplementary **S1**).

In addition to the dose-response curve, we also carried out a time curve using 0.5 and 0.75 mM concentrations. Cells were treated for 30 min, 1, 2, 4, 6, 12 and 24h (Fig. **1C**). It was observed that peptide R18H already shows an antitumor effect after 1h of incubation, and in the period of 24h, the cytotoxic effect was even greater. Therefore, peptide R18H also displays a time dependent effect.

The viability of human melanoma cells lineages after 24h-incubation with R18H (0.06 to 1 mM) was also determined. Untreated cells were incubated in the absence of peptide. As shown in Fig. (**1**), melanoma cells A2058 (Fig**. 1D**), SK-MEL 25 (Fig. **1E**) and A375 (Fig. **1F**) are sensitive to R18H in a dosage dependent
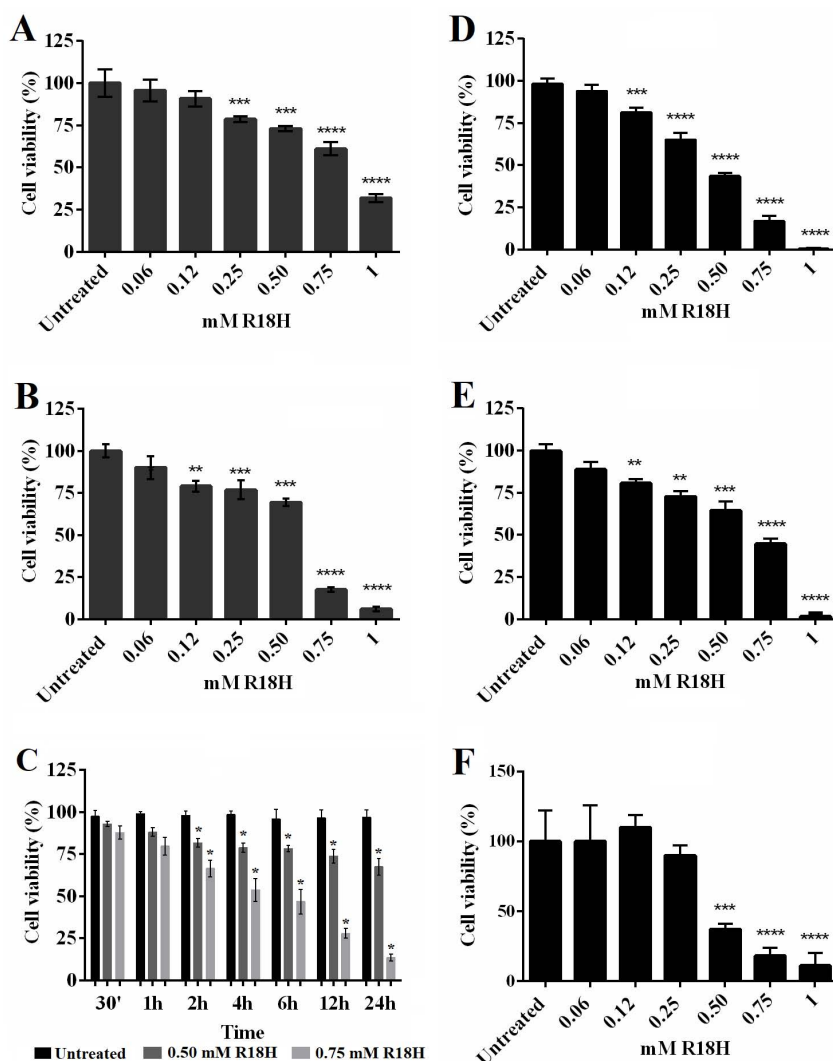
Fig. (1). Cell viability determined by MTT assay. B16F10-Nex2 cells were treated with 0.06; 0.12; 0.25; 0.50; 0.75 and 1.0 mM of R18H peptide for **(A)** 2 hours and **(B)** 24 hours. EC50% in 2h: 0.76 mM; 24h: 0.559 mM. **(C)** B16F10-Nex2 cells were treated with 0.5 and 0.75 mM of R18H for 30 min, 1, 2, 4, 6, 12 and 24h. The viability was determined by MTT assay. Human melanoma cells line A2058 **(D),** SK-MEL 25 **(E)** and A375 **(F)** were treated with 0.06; 0.12; 0.25; 0.50; 0.75 and 1.0 mM of R18H peptide for 24h. Viability was determined by MTT assay or counting cells in a Neubauer chamber with Trypan blue. $*$ p < 0.05; $**$ p< 0.021; $***$ p < 0.005; $****$ p < 0.001.

manner. EC50% values were calculated for A2058 (EC50 = 0.458 mM), SK-KMEL 25 (EC50 = 0.551 mM) and A375 cells (EC50 = 0.536 mM).

We also tested the cytotoxic effect in nontumor cells. HUVEC **(Fig. 2A),** Fibro RP **(Fig. 2B)** and J774 1.6 **(Fig. 2C)** cells line were treated with R18H with 0.5 and 0.7 mM. No cytotoxic effect was observed for HUVEC, Fibro RP and J774 1.6 cells **(Fig. 2A, 2B** and **2C).** In addition, no toxicity was observed for BALB/c mice bone-marrow-derived macrophages treated with R18H at 0.5 mM for 24h. A slight decrease (~10%) in macrophagic viability was detected when cells were incubated with 0.75 mM **(Fig. 2D).** It is worthmentiong that this peptide did not induce hemolysis in red blood cells after 24h **(Fig. 2E).**

3.2. *In vivo* Effect of R18H

After determining the *in vitro* antitumor effects induced by the peptide R18H, we determined the anti-metastatic activity *in vivo* using a syngeneic model with B16F10-Nex2 cells injected intrave-

nously in male C57BL/6 mice. The R18H was administered intraperitoneally for 5 alternate days at 300 μg/day/mouse. After 20 days of inoculation of the B16F10-Nex2 cells, mice were sacrificed and the lungs removed for nodule counting. We observed inhibition in the development of lung nodules of the treated mice when compared to the controls **(Fig. 3** and Supplementary **S2).**

In spite of having a treated mouse that did not respond to the treatment, we observed a decrease of metastatic sites in treated mice when compared with the untreated mice. In addition, the area of lung nodules in the untreated mice was much larger than in the nodules of treated animals (Supplementary **S2).**

After observing the *in vivo* effects of peptide R18H in murine melanoma cells B16F10-Nex2, we examined its toxicity in C57BL/6 mice. Thus, 1 mg of R18H per C57BL/6 mouse was administered i.p. for 3 consecutive days. Two days after the end of treatment mice were sacrificed and heart, lung, spleen, liver, and kidneys removed for histopathology (Supplementary **S3).** The organs of mice treated with 1 mg/day of R18H had no histological
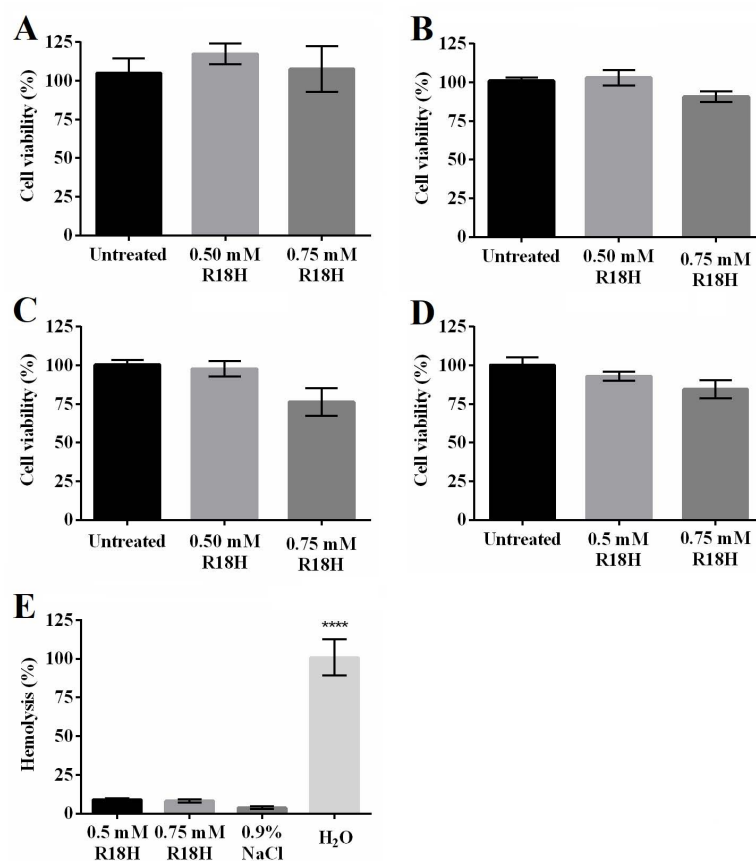
Fig. (2). Viability in non-tumor cell determined by MTT assay. **(A)** HUVEC, **(B)** Fibro RP and **(C)** J774 1.6 cells line were treated with 0.5 mM or 0.75 mM of R18H peptide for 24 hours. **(D)** BALB/c bone-marrow-derived macrophages and the viability was determined by the MTT assay. **(E)** human red blood cells also were treated with 0.5 mM or 0.75 mM of R18H peptide for 24 hours. The supernatant was analyzed by spectrophotometer at 540 nm. As a positive lysis control, red blood cells were resuspended in distilled water (1:20) and a negative control, red blood cells were resuspended in PBS (1:20).

alterations when compared to untreated mice. Therefore, the peptide R18H showed no apparent cytotoxicity such as weight loss, shivering and behavior changes in these animals even when administered with high doses. Moreover, there were no signs of discomfort in the mice throughout the experiments.

3.3. R18H Induces Apoptosis in B16F10-Nex2 Cells

Cells were treated with peptide and DNA degradation checked using the TUNEL Kit. We observed that R18H induces DNA fragmentation in B16F10-Nex2 cells, as detected by intense TUNEL labeling when compared to the untreated cells (Fig. **4A**). After 2 hours treatment with peptide R18H at 0.8 mM, 62.7% of cells presented DNA degradation (Fig. **4Ab**). After 24h treatment at 0.75 mM concentration, 100% of cells displayed DNA degradation, observed by the intense labeling with TUNEL (Fig. **4Ac**). This effect was not observed in untreated cells (Fig. **4Aa**).

To investigate plasma membrane permeabilization in B16F10-Nex2 cells, we visualized PI uptake by fluorescence microscopy (Fig**. 4B**). Cells were treated with 0.8 mM R18H for 2h or 0.75 mM for 24h. After treatment, live cells were stained with PI and as positive control, cells were exposed to 1,000 mM acetic acid for 1h (Fig. **4Bb**). Few cells were positive for PI after 24h treatment (Fig**. 4Bd**). Moreover, no cell was labeled with PI after treatment for 2h with the peptide (Fig. **4Bc**), similarly with untreated cells (Fig. **4Ba**). We observed that PI staining increased from 2h (4.6%) up to 24h (35.8%), compatible with increased plasma membrane perme-

abilization. These data indicate that permeabilization of the plasma membrane is a late apoptosis effect.
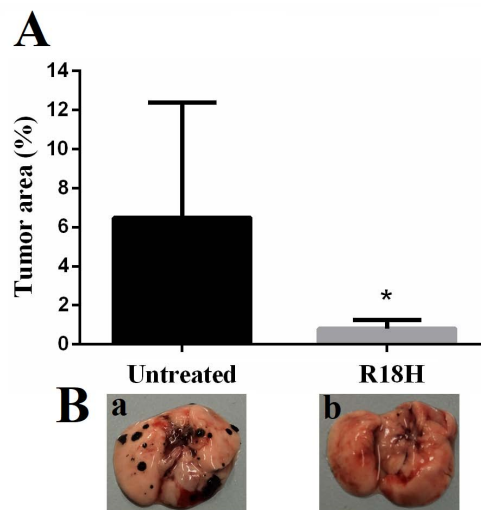

Fig. (3). *In vivo* effect of peptide R18H in the metastatic model. Lung colonization of B16F10-Nex2 cells in a syngeneic system was used to test the protective activity of R18H. **(A)** Protective activity of peptides injected intraperitoneally with doses of 300 μg. Mice (*n* = 5/group) were challenged with 5×10^5 syngeneic B16F10-Nex2 melanoma cells (0.1 ml/mouse). **(B)** Representative images of lungs from untreated and treated animal.
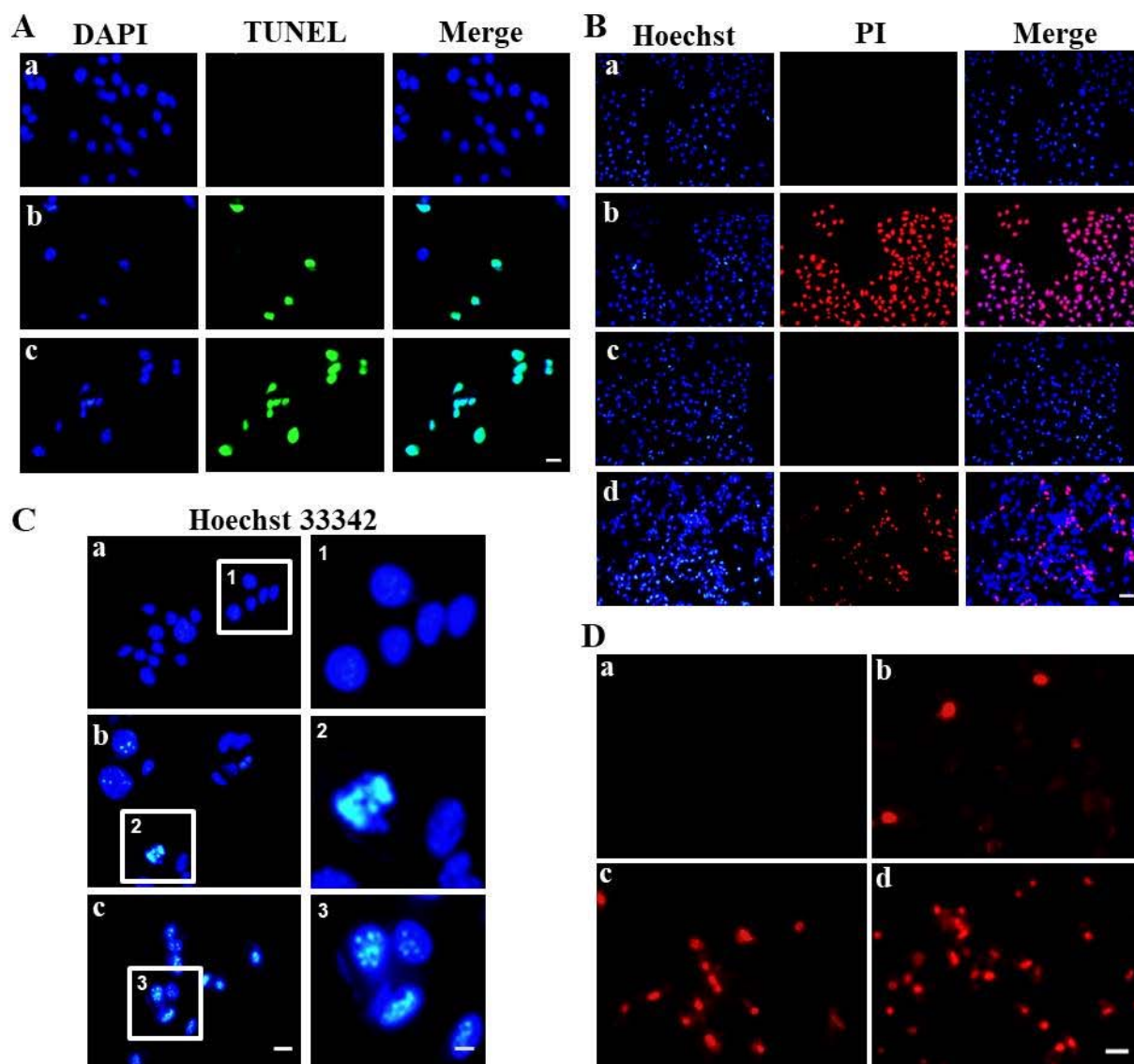
Fig. (4). Degradation of DNA, membrane permeabilization, chromatin condensation and anion superoxide production induced by R18H. (**A**) TUNEL assay in fluorescence microscopy, showing B16F10-Nex2 (**a**) untreated cells, cells treated with R18H at (**b**) 0.8 mM for 2h; (**c**) 0.75 mM for 24 hours. (**B**) (**a**) untreated cells; B16F10-Nex2 cells were treated with (**b**) 1M CH₃COOH as positive control; (**c**) 0.8 mM R18H for 2h; (**d**) 0.75 mM for 24h and stained with DAPI and PI; (**C**) Chromatin condensation seen by Hoechst 33342 staining. B16F10-Nex2 were treated with R18H at (**a**) untreated cells. 1, 2 and 3: 3x magnification. *Scale bars*: 20 and 7 μm (**b**) 0.8 mM for 2 hours; (**c**) 0.75 mM for 24h; (**D**) Anion superoxide produced by B16F10-Nex2 cells treated with (**a**) untreated cells; anion superoxide production detected with DHE. *Scale bar*: 20 μm. Cells were examined under fluorescence microscopy (**b**) positive control with 5mm H₂O₂ cells treated for 2 h with 0,8 mM (**c**); 24 hours with 0,75 mM (**d**).

B16F10-Nex2 cells labeled with Hoechst 33342 displayed chromatin condensation after R18H treatment (Fig. **4C**). Approximately 27% of cells showed chromatin condensation after 2 hours treatment with 0.8 mM R18H (Fig. **4Cb**). As in the TUNEL results, after 24h with 0.75 mM treatment the majority of cells (96%) exhibited chromatin condensation (Fig. **4Cc**). Untreated cells showed no chromatin condensation (Fig. **4Ca**).

Next, we determined whether treated cells presented increased levels of superoxide anion. In the presence of superoxide anion DHE is converted to ethidium that stains cell nuclei in red (Fig. **4D**). It was found that cells treated for 2h (Fig. **4Dc**) or 24 hours (Fig. **4Dd**) showed an increase of 51% and 76% in superoxide anion levels as compared to untreated cells, respectively (Fig. **4Da**); H₂O₂ was used as a positive control (Fig. **4Db**).

To further confirm an apoptotic mechanism triggered by R18H in the B16F10-Nex2 melanoma cell line, cells were incubated with 0.75 mM R18H for 30 min at 37°C and caspases 3, 8 and 9 activation were determined. As shown in Fig. (**5A**), the activities of caspases-3 and -8 were significantly higher in treated cells as compared to untreated cells. Interestingly, no significant increase of caspase-9 activity was detected after R18H treatment (Fig. **5A**). Moreover, we showed that the cytotoxic effect of the peptide was inhibited when cells were incubated with the peptide in the presence of Z-VAD, a pan caspase inhibitor (Fig. **5B**). Additionally, we observed the extracellular release of mitochondrial cytochrome c in treated cells when compared to untreated ones (Fig. **5C**).

In order to confirm the engagement of an apoptotic process we determined the translocation of phosphatidylserine by flow cytome-
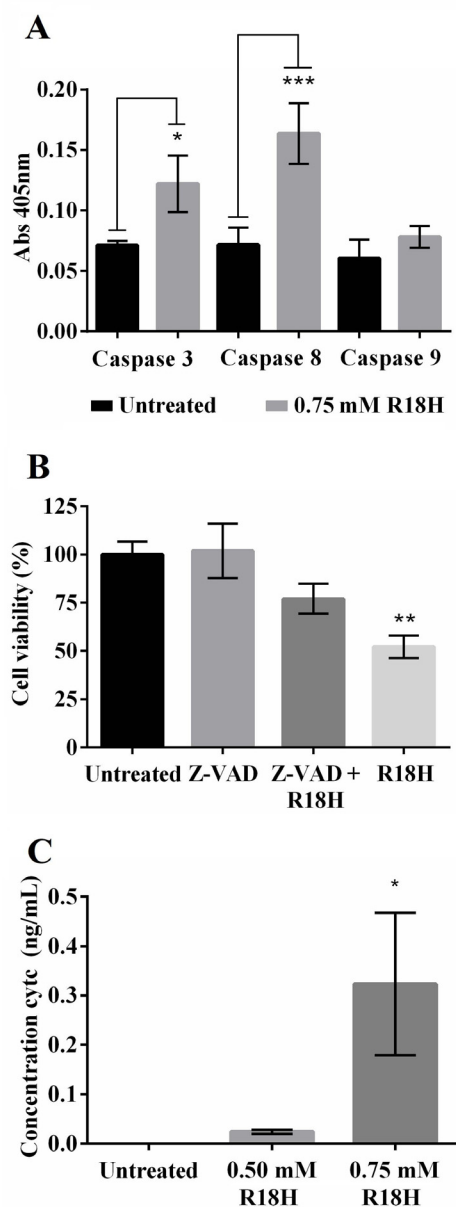
A

B

C

Fig. (5). R18H induces caspases 3 and 8 activation and extracellular release of Cytochrome c. **(A)** B16F10-Nex2 cells incubated with R18H for 30 min induced increased production of caspases 3 and 8 measured by colorimetric assay. **(B)** B16F10-Nex2 cells preincubated with caspase inhibitor and treated with R18H peptide 0.75 mM for 2 hours. **(C)** Release of cytochrome c (cytc) into the extracellular medium after treatment with R18H. * p < 0.05; ** p < 0.021; *** p < 0.005.

try. After treatment with peptide R18H for 2h, annexin V staining reached 14.4% when compared to untreated cells (0.35%). Intense cell staining was also observed by double staining with annexin V and propidium iodide (PI) in cells treated with R18H (55.7%) as compared to untreated ones (2.76%). Furthermore, treated cells staining with propidium iodide alone also increased (0.26%), when compared to untreated cells (2.88%) (Fig. **6A**). Intense annexin V cell staining was also observed after treatment with peptide R18H for 24h (9.57%), when compared with untreated cells (0.67%). The same was seen after double labeling with annexin and propidium iodide (PI) in cells treated with R18H (15.3%) with untreated cells showing reduced staining (3.38%). Treated cells stained only with

propidium iodide also increased (7.6%) when compared to untreated cells (1.28%) (Fig. **6B**).

As evidenced in our results on membrane permeabilization in cells treated with peptide R18H, we also evaluated alternative cell death pathways such as necroptosis or necrosis. For this study, we used necrostatin, a necroptosis reagent that inhibits RIPK1. We observed that R18H-induced cytotoxicity on B16F10-Nex2 was not affected by necrostatin (Supplementary **S4**).

In addition, to discard the possibility that cellular permeabilization could be a necrotic effect, we quantified LDH release by B16F10-Nex2 treated with 0.5 or 0.75 mM R18H. LDH is present in the cytosol and after plasma membrane rupture, a characteristic of necrotic cells, it is released into the extracellular medium. To identify whether R18H caused this disruption, we measured the amount of LDH released into the supernatant of treated cells and observed that it was equivalent to untreated cells, both negligible if compared to the large amounts of LDH detected in effectively lysed B16F10-Nex2 cells (Supplementary **S5**).

Despite the increase in reactive oxygen species levels observed in the above experiment (Fig. **4D**), we did not observe inhibition of the cytotoxic effect of the peptide in presence of ROS inhibitor (N-acetyl L-cysteine) (Supplementary **S6**). Apparently, the increase in ROS levels is due to apoptotic effects in the mitochondria. In fact, we observed the extracellular release of cytochrome c in treated B16F10-Nex2 cells. In order to examine mitochondrial integrity, cells were treated with 0.5 mM R18H for 24h and were analyzed by transmission electron microscopy (Fig. **7**). Significant alterations were identified such as loss of mitochondrial integrity as well as disruption of mitochondrial cristae (Fig **7 e, f, h**, and **i**). Moreover, we also observed chromatin condensation (Fig. **7 d, e, g** and **h**), that had been observed by fluorescence microscopy (Fig. **7B**). None of these alterations were detected in untreated cells (Fig. **7 a, b** and **c**).

3.4. Internalization and Localization of R18H Peptide in B16F10-Nex2 Cells

We used confocal microscopy to examine the internalization and distribution of R18H peptide in B16F10-Nex2 cells. Interestingly, R18H peptide was mainly observed associated with F-actin (Fig. **8A** and **8B**) observed near the cell surface after 30 min treatment and distributed throughout the cytoplasm after 24h. Moreover, we observed that the peptide also colocalized with DAPI in cell nuclei s after 24h (Fig. **8B**).

4. DISCUSSION

Several studies have described peptides with antitumor activity. Specifically, synthetic peptides derived from immunoglobulins induce cell death or inhibit tumor development associated with the induction of apoptosis, autophagy, angiogenesis inhibition and inhibition of cell migration and invasion [8, 9, 13, 32].

Peptides derived from transcription factors may also be promising antitumor agents. Massaoka *et al*. (2014) described that a peptide derived from transcription factor Wilms tumor protein 1 (WT1) reduced the development of metastatic lung nodules, as well as subcutaneous growth of murine melanoma in syngeneic mice. Moreover, the peptide from WT1 also prolonged the survival of nude mice challenged with A2058 melanoma cells. Interestingly, they showed that this peptide induced senescence in B16F10-Nex2 cells and increased expression of p21 and p27 [33]. Wang *et al.* (2017) identified specific peptides that bind to the DNA domain of
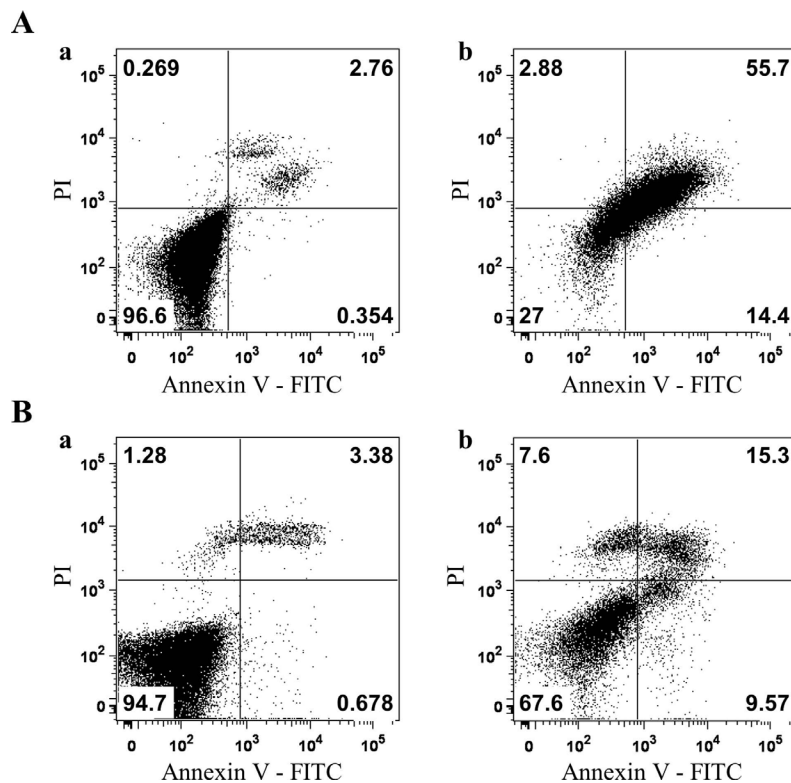
Fig. (6). Phosphatidylserine translocation after the treatment with R18H. **(A)** and **(B)** Phosphatidylserine translocation and membrane permeabilization were determined in B16F10-Nex2 cells treated with **(Ab)** 0.5 mM R18H for 2h **(Bb)** 0.5 mM R18H for 24h, **(Aa)** and **(Ba)** untreated cells. Cells were marked with annexin-V and PI and analyzed by cytometry.
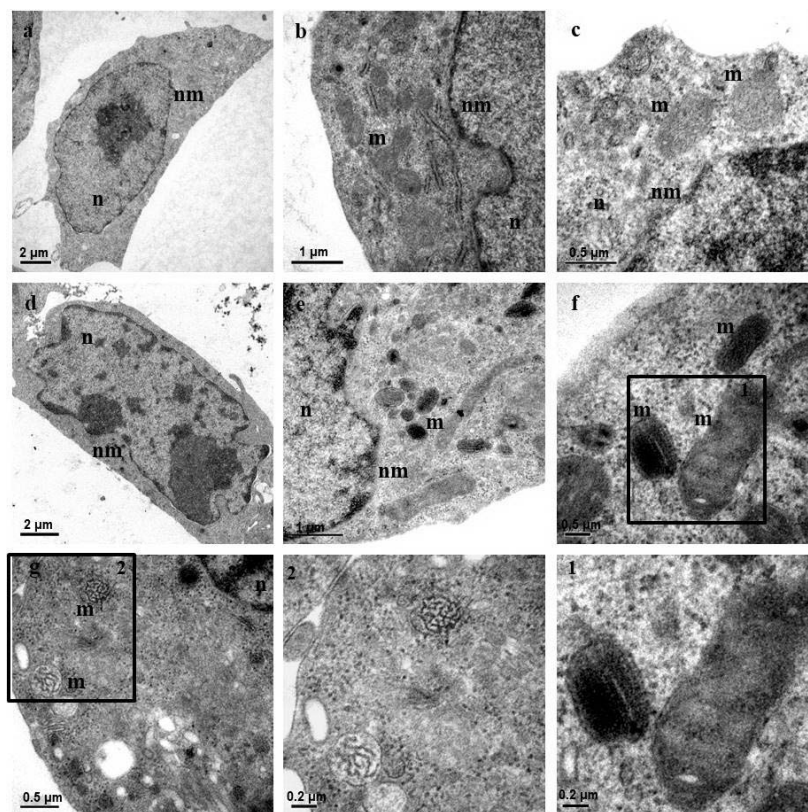

Fig. (7). Morphologic changes in B16F10-Nex2 cells treated with R18H peptide. Transmission electron microscopy of B16F10-Nex2 cells treated with 0.5 mM R18H for 24h. Untreated cells **(a, b and c)** and R18H-treated cells **(d, e, f, g, 1 and 2)**. After the treatment we observed condensed chromatin **(d)**; mitochondria were more electron dense and compact and lacked organized cristae **(e and f)**. Mitochondria (m); Nucleus (n); Nuclear membrane (nm). *Scale bars* are indicated in each image.
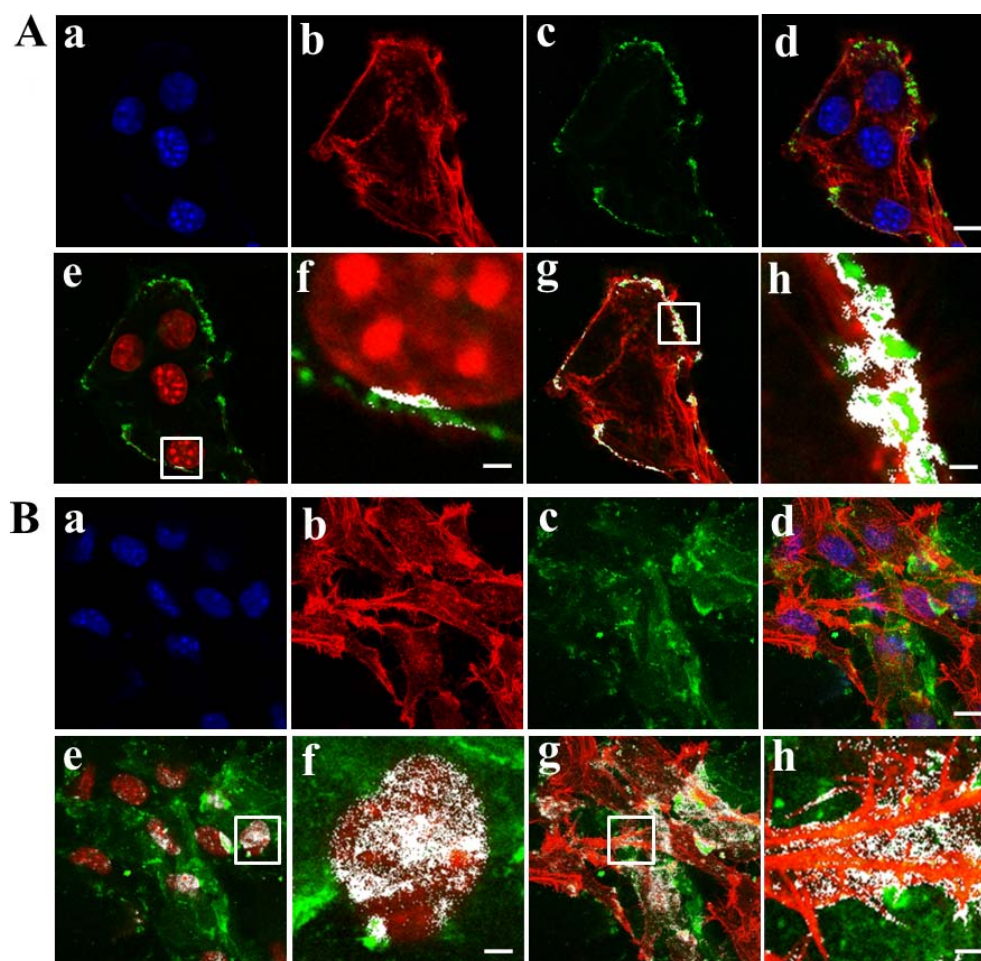
Fig. (8). Internalization of R18H in B16F10-Nex2. B16F10-Nex2 tumor cells were treated with biotinylated R18H for 30 min (**A**) and 24h (**B**), fixed with paraformaldehyde, and permeabilized with Triton X-100. Cells were stained with DAPI (**a**), phalloidin-rhodamine (**b**), streptavidin-AlexaFluor 488 (**c**), and were examined by confocal microscopy; (**d**) *merge*. Co-localization points in white of DAPI (red) with R18H-biotin-Streptavidin-AlexaFluor488 (green) showing co-localization points with nucleus (**e**) and phalloidin-rhodamine (red) and with R18H-biotin-Streptavidin-AlexaFluor 488 (green) showing co-localization points with actin (**g**) in white. White box is a 4x enlargement of e (**f**) and g (**h**). *Scale bar* 20 μm (**a, b, c, d, e, g**), 5 μm (**f, h**). Images were analyzed with Image J. (*The color version of the figure is available in the electronic copy of the article*).

the transcription factor ERG following a decrease in ERG-mediated transcription. These peptides and derived-peptides bound to ERG inducing proteolytic degradation of the ERG protein in prostate cancer. Moreover, they showed that these peptides inhibited cell invasion, proliferation and tumor growth in prostate cancer [34].

The expression of transcription factor BRN2 is strongly upregulated in melanoma cells and this protein is able to proliferation control and melanoma survival [14]. In the present work, we investigated whether peptide R18H derived from transcription factor BRN2 causes antitumor effects *in vitro* and *in vivo* against B16F10-Nex 2 melanoma cells. In fact, developing specific inhibitors of the transcription factor BRN2 could represent an important strategy for growth intervention in developing melanoma at various stages of disease progression [35, 36].

Here we have shown that antitumor activity following treatment with peptide R18H was time- and dose-dependent against murine melanoma B16F10-Nex2 cells. Moreover, the peptide R18H also shown antitumor activity in human melanoma cells lines. No toxicity was observed for nontumor Fibro RP, J774 1.6 and HUVEC cells line. In addition, the peptide was not toxic for BALB/c mice

bone-marrow-derived macrophages and did not induce hemolysis in red blood cells. Also, R18H inhibited the development of pulmonary nodules in metastatic syngeneic mice model. Cytotoxic effects were not observed in unchallenged C57Bl/6 wild-type mice even using a peptide concentration three times higher than the concentration used to treat metastatic melanoma. Our results showed that R18H mechanism of action is related to apoptosis. We observed that this peptide induces DNA degradation, as shown by TUNEL assay, phosphatidylserine translocation, and chromatin condensation, detected by Hoechst 33342 staining and electron microscopy. Additionally, the detection of extracellular release of cytochrome c and caspases 8 and 3 activation [37] after R18H incubation reinforcing the evidence that apoptosis is the death mechanism.

Not only extracellular release of cytochrome c but increased levels of caspases are exclusive events of apoptosis [37]. Moreover, the activation of caspases 8 and 3 in treated cells indicates that the mechanism of peptide R18H-induced cell death might be related to apoptosis. The extracelllar release of cytocrome c is associated with mitochondrial damage. In fact, mitochondrial morphological alterations were identified by electron microscopy in treated cells. Also,

we observed that the peptide induced increased levels of superoxide anions, and that this effect was not reversed by treatment with N-acetyl L-cysteine, a ROS inhibitor. It is well known that the increase in superoxide anion levels from mitochondria as related to apoptosis [38]. Changes in the mitochondrial membrane potential increase ROS concentration with the direct release of cytochrome c from the mitochondria are events related to apoptosis [38-41].

Although classical apoptosis is suggested, we also observed membrane permeabilization of PI after the peptide treatment for 24h. Permeabilization of the plasma membrane is usually associated with death by necrosis or necroptosis [42]. Membrane permeabilization of PI is, however, observed in late apoptosis [43]. To investigate if the permeabilization of the plasma membrane could be raised by necrotic or necroptotic effects, we treated cells with the peptide in the presence of an inhibitor of the necroptosis pathway and observed that the cytotoxic effect of R18H was not reversed by necrostatin, a specific inhibitor of RIPK1 [23, 44, 45]. Moreover, we have shown that the peptide did not promptly release lactate dehydrogenase, characteristic of necrosis [30].

Additionally, an investigation of the peptide internalization and cellular localization was performed by confocal microscopy, showing its nuclear distribution and F-actin co-localization. For instance, we do not know whether this peptide could bind to the DNA binding site and competing with the transcription factor and thereby inducing apoptosis. Also, the interference with actin dynamics and apoptosis induction [9, 13] has yet to be determined. However, these peptide colocalization points with actin (Fig. **8**) could represent peptide being transported to the nucleus. Some studies have shown the participation of actin in transporting intracellular molecules [46-48].

CONCLUSION

The peptide R18H derived from transcription factor BRN2 have antitumor effect *in vitro* and *in vivo*. B16F10-Nex2 melanoma cells present close EC50% values after 2 h (0.76 ± 0.045 mM) and 24h (0.559 ± 0.053 mM) of R18H incubation. The peptide internalizes into tumor cells and its mechanism of action can be explained by the triggering of several apoptotic events. R18H is able to inhibit the development of melanotic lung nodules in mice. Further investigation of peptides displaying antitumor cytotoxic effects should be conducted considering them as alternative therapeutic tools to be associated with conventional anticancer chemotherapy.

ETHICS APPROVAL AND CONSENT TO PARTICIPATE

All experimental protocols using C57BL/6 mice were approved by Ethics Committee for Animal Experimentation of the University of Mogi das Cruzes (11/015), Brazil. The experimental protocol using BALB/c mice was approved by the Ethical Committee for Animal Experimentation of the Biology Institute of UNICAMP (#4535-1/2017), Brazil.

HUMAN AND ANIMAL RIGHTS

No humans were used in this study, The reported experiments on animals were in accordance with the standards set forth in the 8th Edition of Guide for the Care and use of Laboratory Animals (http//grants.nih.gov/grants/olaw/Guide-for-the-care-and-useoflaboratory-animals.pdf) published by the National Academy of Sciences, The National Academies Press, Washington DC, United States of America.

CONSENT FOR PUBLICATION

Not applicable.

CONFLICT OF INTEREST

The authors declare no conflict of interest, financial or otherwise.

SUPPLEMENTARY MATERIAL

Supplementary material is available on the publisher's website along with the published article.

REFERENCES

[1]   American Cancer Society. Melanoma Skin Cancer. https://www. cancer.org/cancer/melanoma-skin-cancer/about/key-statistics.html/ (Accessed August 03, **2018**).

[2]   World Health Organization. Health effects of UV radiation http://www.who.int/uv/health/uv_health2/en/index1.html/ (Accessed August 03, **2018**).

[3]   Block, K.I.; Gyllenhaal, C.; Lowe, L.; Amedei, A.; Amin, A.R.M.R.; Amin, A.; Aquilano, K.; Arbiser, J.; Arreola, A.; Arzumanyan, A.; Ashraf, S.S.; Azmi, A.S.; Benencia, F.; Bhakta, D.; Bilsland, A.; Bishayee, A.; Blain, S.W.; Block, P.B.; Boosani, C.S.; Carey, T.E.; Carnero, A.; Carotenuto, M.; Casey, S.C.; Chakrabarti, M.; Chaturvedi, R.; Chen, G.Z.; Chen, H.; Chen, S.; Chen, Y.C.; Choi, B.K.; Ciriolo, M.R.; Coley, H.M.; Collins, A.R.; Connell, M.; Crawford, S.; Curran, C.S.; Dabrosin, C.; Damia, G.; Dasgupta, S.; DeBerardinis, R.J.; Decker, W.K.; Dhawan, P.; Diehl, A.M.E.; Dong, J.T.; Dou, Q.P.; Drew, J.E.; Elkord, E.; El-Rayes, B.; Feitelson, M.A.; Felsher, D.W.; Ferguson, L.R.; Fimognari, C.; Firestone, G.L.; Frezza, C.; Fujii, H.; Fuster, M.M.; Generali, D.; Georgakilas, A.G.; Gieseler, F.; Gilbertson, M.; Green, M.F.; Grue, B.; Guha, G.; Halicka, D.; Helferich, W.G.; Heneberg, P.; Hentosh, P.; Hirschey, M.D.; Hofseth, L.J.; Holcombe, R.F.; Honoki, K.; Hsu, H.Y.; Huang, G.S.; Jensen, L.D.; Jiang, W.G.; Jones, L.W.; Karpowicz, P.A.; Keith, W.N.; Kerkar, S.P.; Khan, G.N.; Khatami, M.; Ko, Y.H.; Kucuk, O.; Kulathinal, R.J.; Kumar, N.B.; Kwon, B.S.; Le, A.; Lea, M.A.; Lee, H.Y.; Lichtor, T.; Lin, L.T.; Locasale, J.W.; Lokeshwar, B.L.; Longo, V.D.; Lyssiotis, C.A.; MacKenzie, K.L.; Malhotra, M.; Marino, M.; Martinez-Chantar, M.L.; Matheu, A.; Maxwell, C.; McDonnell, E.; Meeker, A.K.; Mehrmohamadi, M.; Mehta, K.; Michelotti, G.A.; Mohammad, R.M.; Mohammed, S.I.; Morre, D.J.; Muralidhar, V.; Muqbil, I.; Murphy, M.P.; Nagaraju, G.P.; Nahta, R.; Niccolai, E.; Nowsheen,

S.; Panis, C.; Pantano, F.; Parslow, V.R.; Pawelec, G.; Pedersen, P.L.; Poore, B.; Poudyal, D.; Prakash, S.; Prince, M.; Raffaghello, L.; Rathmell, J.C.; Rathmell, W.K.; Ray, S.K.; Reichrath, J.; Rezazadeh, S.; Ribatti, D.; Ricciardiello, L.; Robey, R.B.; Rodier, F.; Rupasinghe, H.P.V.; Russo, G.L.; Ryan, E.P.; Samadi, A.K.; Sanchez-Garcia, I.; Sanders, A.J.; Santini, D.; Sarkar, M.; Sasada, T.; Saxena, N.K.; Shackelford, R.E.; Shantha-Kumara, H.M.C.; Sharma, D.; Shin, D.M.; Sidransky, D.; Siegelin, M.D.; Signori, E.; Singh, N.; Sivanand, S.; Sliva, D.; Smythe, C.; Spagnuolo, C.; Stafforini, D.M.; Stagg, J.; Subbarayan, P.R.; Sundin, T.; Talib, W.H.; Thompson, S.K.; Tran, P.T.; Ungefroren, H.; Vander-Heiden, M.G.; Venkateswaran, V.; Vinay, D.S.; Vlachostergios, P.J.; Wang, Z.; Wellen, K.E.; Whelan, R.L.; Yang, E.S.; Yang, H.; Yang, X.; Yaswen, P.; Yedjou, C.; Yin, X.; Zhu, J.; Zollo, M. Designing a broad-spectrum integrative approach for cancer prevention and treatment. *Semin. Canc. Biol.*, **2015**, *35*, S276-S304.

[4]   Röckmann, H.; Schadendorf, D. Drug resistance in human melanoma: Mechanisms and therapeutic opportunities. *Onkologie*, **2003**, *26*, 581-587.

[5]   Soengas, M.S.; Lowe, S.W. Apoptosis and melanoma chemoresistance. *Oncogene*, **2003**, *22*(20), 3138-3151.

[6]   Sookraj, K.A.; Adler, V.; Sarafraz-Yazdi, E.; Bowne, W.B. W1961 Novel p53-derived peptide induces extensive necrosis in cancer cells. *Gastroenterology*, **2008**, *134*(4), 7743.

[7]   Fulda, S.; Wick, W.; Weller, M.; Debatin, K.M. Smac agonists sensitize for Apo2L/TRAIL-or anticancer drug-induced apoptosis and induced regression of malignant glioma *in vivo*. *Nat. Med.*, **2002**, *8*(8), 808-815.

[8]   Polonelli, L.; Pontón, J.; Elguezabal, N.; Moragues, M.D.; Casoli, C.; Pilotti, E.; Ronzi, P.; Dobroff, A.S.; Rodrigues, E.G.; Juliano, M.A.; Maffei, D.L Antibody Complementarity-Determining Regions (CDRs) can display differential antimicrobial, antiviral and antitumor activities. *PLoS One*, **2008**, *3*(6), 2371.

[9]   Arruda, D.C.; Santos, L.C.P.; Melo, F.M.; Pereira, F.V.; Figueiredo, C.R.; Matsuo, A.L.; Mortara, R.A.; Juliano, M.A.; Rodrigues, E.G.; Dobroff, A.S.; Polonelli, L.; Travassos, L.R. β-Actin-binding complementarity-determining region 2 of variable heavy chain from monoclonal antibody C7 induces apoptosis in several human tumor cells and is protective against metastatic melanoma. *J. Biol. Chem.*, **2012**, *287*(18), 14912-14922.

[10]   Maijaroen, S.; Jangpromma, N.; Daduang, J.; Klaynongsruang, S. KT2 and RT2 modified antimicrobial peptides derived from Crocodylus siamensis Leucrocin I show activity against human colon cancer HCT-116 cells. *Environ. Toxicol. Pharmacol.*, **2018**, *62*, 164-176.

[11]   Feng, Z.; Wang, H.; Du, X.; Shi, J.; Li, J.; Xu, B. Minimal C-terminal modification boosts peptide self-assembling ability for necroptosis of cancer cells. *Chem. Commun. (Camb)*, **2016**, *52*(37), 6332-6335.

[12]   Krause, G.C.; Lima, K.G.; Dias, H.B.; Da-Silva, E.F.G.; Haute, G.V.; Basso, B.S.; Gassen, R.B.; Marczak, E.S.; Nunes, R.S.B.; De-Oliveira, J.R. Liraglutide, a glucagon-like peptide-1 analog, induce autophagy and senescence in HepG2 cells. *Eur. J. Pharmacol.*, **2017**, *15*, 809, 32-41.

[13]   Rabaça, A.N.; Arruda, D.C.; Figueiredo, C.R.; Massaoka, M.H.; Farias, C.F.; Tada, D.B.; Maia, V.C.; Silva, Jr. P.I.; Girola, N.; Real, F.; Mortara, R.A.; Polonelli, L.; Travassos, L.R. AC-1001 H3 CDR peptide induces apoptosis and signs of autophagy *in vitro* and exhibits antimetastatic activity in a syngeneic melanoma model. *FEBS Open Bio.*, **2016**, *6*(9), 885-901.

[14]   Cook, A.L.; Sturm, R.A. POU domain transcription factors: BRN2 as a regulator of melanocytic growth and tumourigenesis. *Pigm. Cell Melanoma Res.*, **2008**, *21*(6), 611-626.

[15]   Goodall, J.; Wellbrock, C.; Dexter, T.J.; Roberts, K.; Marais, R.; Goding, C.R. The BRN2 transcription factor links activated BRAF to melanoma proliferation. *Mol. Cell Biol.*, **2004**, *24*, 2923-2931.

[16]   Wellbrock, C.; Rana, S.; Paterson, H.; Pickersgill, H.; Brummelkamp, T.; Marais, R. Oncogenic BRAF regulates melanoma proliferation through the lineage specific factor MITF. *PLoS One*, **2008**, *163*(7), e2734 15.

[17]   Fane, M.E.; Chhabra, Y.; Smith, A.G.; Sturm, R.A. BRN2, a POUerful driver of melanoma phenotype switching and metastasis. *Pigment Cell Melanoma Res.*, **2019**, *32*, 9-24.

[18]   Goodall, J.; Carreira, S.; Denat, L.; Kobi, D.; Davidson, I.; Nuciforo, P.; Sturm, R.; Larue, L.; Goding, C.R. BRN2 represses microphthalmia-associated transcription factor expression and marks

a distinct subpopulation of microphthalmia-associated transcription factor-negative melanoma cells. *Cancer Res.*, **2008**, *68*(19), 7788-7794.

[19]   Bonvin, E.; Falletta, P.; Shaw, H.; Delmas, V.; Goding, C.R. A phosphatidylinositol 3-kinase-Pax3 axis regulates BRN2 expression in melanoma. *Mol. Cell Biol.*, **2012**, *32*(22), 4674-4683.

[20]   Dobroff, A.S.; Rodrigues, E.G.; Moraes, J.Z.; Travassos, L.R. Protective anti-tumor monoclonal antibody recognizes a conformational epitope similar to melibiose at the surface of invasive murine melanoma cells. *Hybrid. Hybridomics*, **2002**, *21*, 321-331.

[21]   Miguel, D.C.; Flannery, A.R.; Mittra, B.; Andrews, N.W. Heme uptake mediated by LHR1 is essential for *Leishmania amazonensis* virulence. *Infect. Immun*., **2013**, *81*(10), 3620-3626.

[22]   Oddo, A.; Hansen, P.R. Hemolytic activity of antimicrobial peptides. *Methods Mol. Biol.*, **2017**, *1548*, 427-435.

[23]   Atkinson, E.A.; Barry, M.; Darmon, A.J.; Shostak, I.; Turner, P.C.; Moyer, R.W.; Bleackley, R.C. Cytotoxic T lymphocyte-assisted suicide. Caspase 3 activation is primarily the result of the direct action of granzyme B. *J. Biol. Chem.*, **1998**, *273*(33), 21261-21266.

[24]   Dong, T.; Liao, D.; Liu, X.; Lei, X. Using small molecules to dissect non-apoptotic programmed cell death: Necroptosis, ferroptosis, and pyroptosis. *Chembiochem*, **2015**, *16*(18), 2557-2561.

[25]   Figueiredo, C.R.; Matsuo, A.L.; Pereira, F.V.; Rabaça, A.N.; Farias, C.F.; Girola, N.; Massaoka, M.H.; Azevedo, R.A.; Scutti, J.A.; Arruda, D.C.; Silva, L.P.; Rodrigues, E.G.; Lago, J.H.; Travassos, L.R.; Silva, R.M. *Pyrostegia venusta* heptane extract containing saturated aliphatic hydrocarbons inducesapoptosis on B16F10-Nex2 melanoma cells and displays antitumor activity *in vivo*. *Pharmacogn. Mag.*, **2014**, *10*(Suppl 2), S363-376.

[26]   Negoescu, A.; Guillermet, C.; Lorimier, P.; Brambilla, E.; Labat-Moleur, F. Importance of DNA fragmentation in apoptosis with regard to TUNEL specificity. *Biomed. Pharmacother.*, **1998**, *52*(6), 252-258.

[27]   Amin, H.M.; Medeiros, L.J.; Ma, Y.; Feretzaki, M.; Das, P.; Leventaki, V.; Rassidakis, G.Z.; O'Connor, S.L.; McDonnell, T.J.; Lai, R. Inhibition of JAK3 induces apoptosis and decreases anaplastic lymphoma kinase activity in anaplastic large cell lymphoma. *Oncogene*, **2003**, *22*(35), 5399-5407.

[28]   Kuypers, F.A.; Lewis, R.A.; Hua, M.; Schott, M.A.; Discher, D.; Ernst, J.D.; Lubin, B.H. Detection of altered membrane phospholipid asymmetry in subpopulations of human red blood cells using fluorescently labeled annexin V. *Blood*, **1996**, *87*(3), 1179-1187.

[29]   Thornberry, N.A.; Lazebnik, Y. Caspases: Enemies within. *Science*, **1998**, *281*(5381), 1312-1316.

[30]   Sinthujaroen, P.; Wanachottrakul, N.; Pinkaew, D.; Petersen, J.R.; Phongdara, A.; Sheffield-Moore, M.; Fujise, K. Elevation of serum fortilin levels is specific for apoptosis and signifies cell death *in vivo*. *BBA Clin.*, **2014**, *2*, 103-111.

[31]   Chan, F.K.; Moriwaki, K.; De-Rosa, M.J. Detection of necrosis by release of lactate dehydrogenase activity. *Methods Mol. Biol.*, **2013**, *979*, 65-70.

[32]   Girola, N.; Matsuo, A.L.; Figueiredo, C.R.; Massaoka, M.H.; Farias, C.F.; Arruda, D.C.; Azevedo, R.A.; Monteiro, H.P.; Resende-Lara, P.T.; Cunha, R.L.; Polonelli, L.; Travassos, L.R. The Ig VH complementarity-determining region 3-containing Rb9 peptide, inhibits melanoma cells migration and invasion by interactions with Hsp90 and an adhesion G-protein coupled receptor. *Peptides*, **2016**, *85*, 1-15.

[33]   Massaoka, M.H.; Matsuo, A.L.; Figueiredo, C.R.; Girola, N.; Faria, C.F.; Azevedo, R.A.; Travassos, L.R. A novel cell-penetrating peptide derived from WT1 enhances p53 activity, induces cell senescence and displays antimelanoma activity in xeno- and syngeneic systems. *FEBS Open Bio.*, **2014**, *21*(4), 153-161.

[34]   Wang, X.; Qiao, Y.; Asangani, I.A.; Ateeq, B.; Poliakov, A.; Cieślik, M.; Pitchiaya, S.; Chakravarthi, B.V.; Cao, X.; Jing, X.; Wang, C.X.; Apel, I.J.; Wang, R.; Tien, J.C.; Juckette, K.M.; Yan, W.; Jiang, H.; Wang, S.; Varambally, S.; Chinnaiyan, A.M. Development of peptidomimetic inhibitors of the ERG gene fusion product in prostate cancer. *Canc. Cell*, **2017**, *31*(4), 532-548.

[35]   Peixoto, P.; Liu, Y.; Depauw, S.; Hildebrand, M.P.; Boykin, D.W.; Bailly, C.; Wilson, W.D.; David-Cordonnier, M.H. Direct inhibition of the DNA-binding activity of POU transcription factors Pit-1 and Brn-3 by selective binding of a phenyl-furanbenzimidazole dication. *Nucleic Acids Res.*, **2008**, *36*, 3341-3353.

[36]   Pathria, G.; Ronai, Z.A. BRN 2 Invade. *Cancer Cell*, **2018**, *34*(1), 1-3.

[37]   Renz, A.; Berdel, W.E.; Kreuter, M.; Belka, C.; Schulze-Osthoff, K.; Los, M. Rapid extracellular release of cytochrome c is specific for apoptosis and marks cell death *in vivo. Blood,* **2001,** *98,* 1542-1548.

[38]   Gobe, G.; Crane, D. Mitochondria, reactive oxygen species and cadmium toxicity in the kidney. *Toxicol. Lett.,* **2010,** *198*(1), 49-55.

[39]   Luetjens, C.M.; Kögel, D.; Reimertz, C.; Düßmann, H.; Renz, A.; Schulze-Osthoff, K.; Nieminen, A.L.; Poppe, M.; Prehn, J.H. Multiple kinetics of mitochondrial cytochrome c release in drug-induced apoptosis. *Mol. Pharmacol.,* **2001,** *60,* 1008-1019.

[40]   Paradies, G.; Petrosillo, G.; Pistolese, M.; Ruggiero, F.M. Reactive oxygen species affect mitochondrial electron transport complex I activity through oxidative cardiolipin damage. *Gene,* **2002,** *286,* 135-141.

[41]   Vakifahmetoglu-Norberg, H.; Ouchida, A.T.; Norberg, E. The role of mitochondria in metabolism and cell death. *Biochem. Biophys. Res. Commun.,* **2017,** *482*(3), 426-431.

[42]   Masse, M.; Glippa, V.; Saad, H.; Le Bloas, R.; Gauffeny, I.; Berthou, C.; Czjzek, M.; Cormier, P.; Cosson, B. An eIF4E-interacting peptide induces cell death in cancer cell lines. *Cell Death Dis.,* **2014,** *5*(10), e1500.

[43]   Franz, S.; Frey, B.; Sheriff, A.; Gaipl, U.S.; Beer, A.; Voll, R.E.; Kalden, J.R.; Herrmann, M. Lectins detect changes of the glycosylation status of plasma membrane constituents during late apoptosis. *Cytometry A.,* **2006,** *69,* 230-239.

[44]   Sun, L.; Wang, H.; Wang, Z.; He, S.; Chen, S.; Liao, D.; Wang, L.; Yan, J.; Liu, W.; Lei, X.; Wang, X. Mixed lineage kinase domain-like protein mediates necrosis signaling downstream of RIP3 kinase. *Cell,* **2012,** *148*(1-2), 213-227.

[45]   Sun, L.; Wang, H.; Wang, Z.; He, S.; Chen, S.; Liao, D.; Wang, L.; Yan, J.; Liu, W.; Lei, X.; Wang, X. Mixed lineage kinase domain-like protein MLKL causes necrotic membrane disruption upon phosphorylation by RIP3. *Mol. Cell,* **2014,** *148*(1), 213-227.

[46]   Asaro, R.J.; Zhu, Q.; Cabrales, P.; Carruthers, A. Do skeletal dynamics mediate sugar uptake and transport in human erythrocytes? *Biophys. J.,* **2018,** *114*(6), 1440-1454.

[47]   Shamloo, A.; Mehrafrooz, B. Nanomechanics of actin filament: A molecular dynamics simulation. *Cytoskeleton,* **2018,** *75*(3), 118-130.

[48]   He, L.; Sayers, E.J.; Watson, P.; Jones, A.T. Contrasting roles for actin in the cellular uptake of cell penetrating peptide conjugates. *Sci. Rep.,* **2018,** *8*(1), 7318.